Thickness Induced Structural Transition in Suspended fcc Metal Nanofilms

Anwar Hasmy and Ernesto Medina

Laboratorio de Física Estadística de Sistemas Desordenados, Centro de Física, IVIC, Apartado 21827, Caracas 1020A, Venezuela

(Received 18 January 2000; published 13 February 2002)

Recent experiments show that at a critical thickness, surface forces can dominate the bulk coercing suspended Au nanofilms to globally reconstruct from the (001) to the (111) orientation. Here we perform molecular dynamics simulations demonstrating that such transformations are generic to other fcc metals. This contrasts with surface reconstruction on the bulk occurring only in 5*d* metals. We show that this phenomenon occurs once a small energy barrier is overcome and discuss the relation of such a barrier and the critical thickness to film surface area and boundary conditions.

DOI: 10.1103/PhysRevLett.88.096103 PACS numbers: 68.35.Bs, 61.50.Ks, 61.66.Bi

Without doubt, the next decades will evidence major advances in nanotechnology, made possible by new developments in the manipulation and control of materials at the atomic scale. As one attempts to give ever smaller clumps of matter convenient shapes to fit device purposes, one meets an intrinsic limit to design given by the stability of the resulting structure [1]. In atomic clusters, shell/supershell phenomena determine the shape and numbers of atoms that are strongly preferred energetically [2–4]. Other examples of systems with particular stable configurations correspond to gold nanowires [5–8]. Recently it has been established that during nanocontact formation, special stable structures (with "magic" numbers of atoms) spontaneously arise and determine contact geometry [9,10], thus constraining nanostructure design. Another design element is the use of thin films where reconstructions of a newly exposed surface determines what and how overlayers can be grown on it [11].

It is well established that many (001) oriented surfaces of fcc metals on a substrate reconstruct to a contracted, quasihexagonal, close packed layer [12–15]. The driving force for the reconstruction is a reduction of the surface energy enough to compensate for the ensuing mismatch strain. Similar reconstructions apply to the (001) facet of small gold clusters [16], and the hexagonal surface reconstruction of gold nanowires [5]. Nevertheless, surface reconstruction on a substrate in fcc metals is by no means spontaneous and favored. In fact, it is observed that stress overcomes the substrate resistance to produce spontaneous reconstructions only in 5*d* metals (Ir, Pt, Au), whereas in 4*d* metals (Rh, Pd, Ag) external stress must be applied [12]. Reconstruction can also be induced by increasing temperature as in heterogeneous adsorbate-substrate systems [17]. For freestanding or suspended metallic films, surface stress should become increasingly comparable to the remaining bulk forces as film width shrinks. Recently, it has been suggested that such a tendency drives striking filmwide reconstructions in gold nanofilms [18]. The initial gold (001) oriented film is made by vacuum deposition, and a local thinning process is performed by electron beam irradiation. When the irradiated region becomes very thin, 2–3 nm, the film spontaneously transforms into the (111) orientation.

In this Letter we describe molecular dynamics (MD) simulations showing that filmwide reconstruction is a universal phenomenon in transition metals including both 5*d* and 4*d*. Isokinetic-isobaric MD simulations show that this transition can take place in spite of the presence of fixed (001) oriented borders that constrain changes in the irradiated (thinned) region of the experimental sample. In this work, we consider the embedded atom method and the corresponding state of the art embedding functions [13,14,19], able to fit bulk and surface properties. This method has been shown to be accurate in describing both reconstructions and diffusion on metal surfaces [13,14,20] as well as metallic nanocontact formation of even a few atoms [21,22]. On the other hand, it is specially adapted to relatively large structures, out of the reach of *ab initio* methods.

Energy minimization of freestanding films with periodic boundary conditions (PBC) was performed by considering atoms on a fcc lattice with exposed surfaces in the (001), (011), and (111) directions. By an isotropic expansion of the whole sample, the distance between these atoms is discretely varied, computing for each situation, the average cohesive energy over all atoms. The energy curve, as a function of the expanded distance, exhibits a minimum E_m at a given lattice constant a^*, smaller than the bulk due to the expected contraction [23]. Figure 1a shows E_m as a function of the number of layers N_l for orientations (111), (011), and (001) of Au fcc films with PBC in the xy plane (film plane). The local electron density and the pairwise potential decay roughly exponentially with the interatomic distance, and their influence is cutoff at approximately second nearest neighbors. Thus, PBC simulate an effectively infinite system. Note that the curve for the (111) orientation is always energetically favored, in comparison with the other orientations. For large N_l values, all curves will tend to the bulk cohesive energy (-3.93 eV for Au). Similar results are obtained for Ag, Al, Ni, and Pt films (data not shown), suggesting the geometrical nature of the effect, independent of the specific shape of the interaction potential.

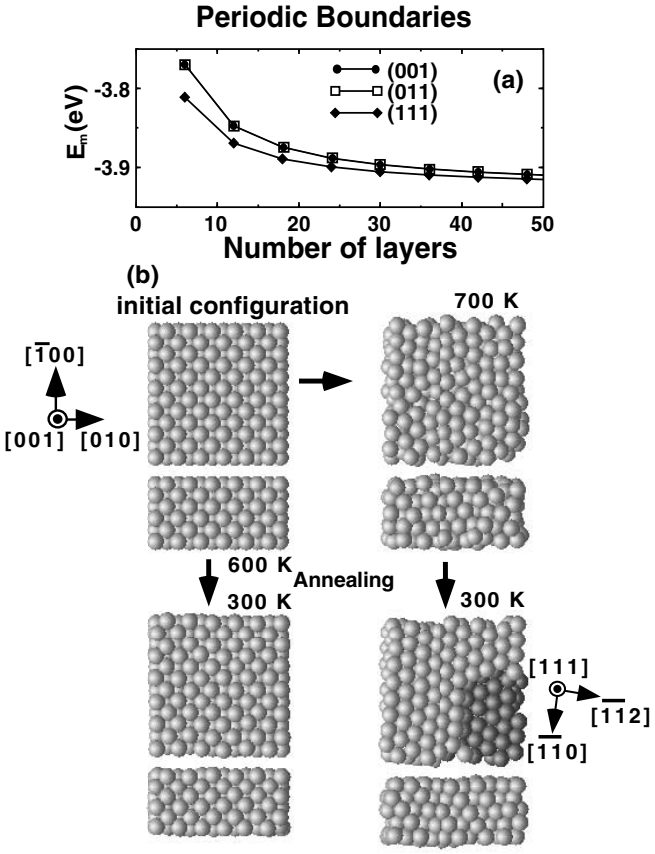

FIG. 1. (a) The energy minimum E_m versus the number of Au film layers for the indicated orientations, and (b) typical molecular dynamics configurations of Au films. Periodic boundary conditions in the xy plane (film plane) are considered. Depicted films correspond initially to the (001) orientation comprising six layers (top left), and the resulting structures after an annealing procedure from 600 and 700 K to 300 K (see text). We show the Au film plane (above) and lateral (below) views, illustrating the layer by layer structure. Axis orientations are indicated for the original and transformed films.

Nevertheless, if one starts from a (001) orientation, the low energy state (111) may be unreachable depending on the available thermal energy scale due to energy barriers between the stable and metastable configurations. In order to address this issue, we performed temperature controlled molecular dynamics simulations accompanied with a regular annealing procedure.

We considered a (001) film with six layers with PBC in the xy planes at a local energy minimum. Annealing is performed by heating the system at a given temperature T_{ann}, and then gradually cooling, at a rate of 1 K/10^{-11} sec, with a 10^{-14} sec integration step, until $T = 300$ K. The film is heated in order to overcome the energy barrier towards a stable minimum energy. For the system with six layers (72 atoms each layer) and departing from a temperature $T_{\text{ann}} \leq 600$ K, film MD configurations do not exhibit changes in their initial orientation (001) as observed in Fig. 1b (bottom left panel). However, starting at $T_{\text{ann}} \geq 700$ K the film undergoes a structural transition (bottom right panel): every layer reconstructs to a hexagonal close packed structure with an fcc stacking (secondary layer depicted as darker spheres). Correlation function analysis, of the resulting structure, was characteristic of the Au bulk fcc system with a small amount of fluctuations mainly due to the filmwide corrugation (bottom right panel). The above analysis also evidenced a sample contraction of approximately 5%. Such corrugation and contraction is similar to that observed in typical 5×1 surface reconstruction [12], but here it takes place on the whole sample. Note that the transformed structure consists of five layers due to the increased inlayer density as compared to the original, locally stable, six layered structure.

Motivated by experiments of Kondo *et al.* [18] on finite systems, energy minimization was also computed for Au films in their different (111), (011), and (001) orientations with *free boundary conditions*. Figure 2 shows results for films of different thickness N_l and surface areas. From the bottom up, the curves correspond to surface areas (in number of atoms), N_a, of 36, 72, and 200 atoms. Note that, for the largest number of layers, the (001) orientation has a lower energy, while for thinner samples, the (111) orientation becomes energetically favored defining a critical number of layers N_l^*. The intersection point N_l^*, of the energy curves, increases with surface area (see arrows in Fig. 2). For Au, N_l^* versus N_a data can be fitted quite well by the expression $N_l^* \approx \sqrt{2N_a}$. This fit can be seen as the relation between the number of surface atoms versus the number of bulk layers in a fcc metal (two atoms per surface plaquette and two layers per primitive cell) where one gets the relation $N_l^* = \sqrt{2N_a} + 1$. This means that, as one goes to samples below cubic proportions, we have a new global minimum in which the film orientation is (111). Calculations in other $4d$ and $5d$ transition metal films show similar results. Such conclusion is consistent with the observed (111) preferred orientation of electrodeposited Ni pillar nanomagnet arrays [24].

The simulations show that the thinning process results in a structural transition, from the (001) to the (111) orientation, when the sample dimensions are 8×36, 11×72, and 17×200 (see Fig. 2). These values correspond to $\sim$1.3–3 nm in thickness, which agree with Au nanofilm experiments, in spite of the omission, at this point, of realistic boundary conditions. The latter agreement suggests that perimeter strain effects claimed in Ref. [18], due to the mismatch between the (001) region and the transformed (111) region are already negligible for our sample dimensions and thus is not a decisive factor determining the critical thickness. In fact, as we show below, the strain energy only tunes the energy barrier between the minima of the (001) and (111) configurations.

For an estimation of the energy barriers between (001) and (111) finite freestanding Au films, taking into account the (001) oriented border constraints (due to the bulk unthinned film, in the real experimental situation of Kondo *et al.*), an isobaric-isokinetic molecular dynamics

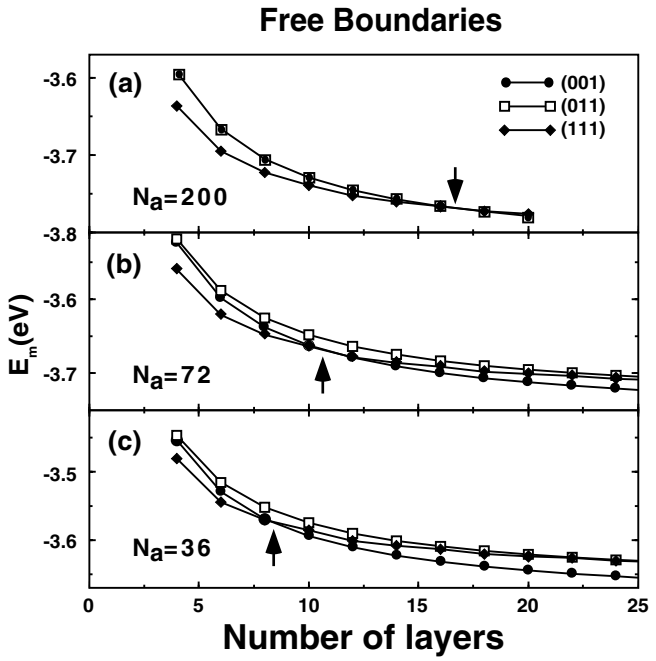

FIG. 2. Minimum energy as a function of the number of layers for Au films of different orientations and finite area. Each layer contains (a) 200, (b) 72, and (c) 36 atoms (N_a). The arrows indicate the number of layers below which the (111) orientation becomes preferred energetically.

procedure is used. The integration is done by a fourth order predictor-corrector method with a 10^{-15} sec time step. The implemented method for pressure control and isotropic volume fluctuations corresponds to a modified Andersen scheme. We considered a cylindrical geometry where the external annular region has an fcc crystalline structure with a (001) surface orientation perpendicular to the cylinder axis. Within this annulus we place a cylindrical test film with a given number of layers. The thermal energy of atoms in the annulus is ignored (i.e., these atoms are frozen), but they can move with the whole sample due to the kinetic volume energy as required by the constant pressure constraint. The isotropic volume contraction is limited only by the core-core repulsion between annular frozen atoms at the borders of the nanofilm.

In Fig. 3 we present a cut of the first configuration at time equal to 0. Gold (top layer) and white (secondary layer) atoms correspond to mobile atoms. Darker atoms in the annulus have a fixed lattice arrangement subject only to contraction controlled by the isobaric MD. The initial Au film diameter is approximately 5 nm (corresponding to the nonfrozen atoms region), much larger than their thickness 1.4–3.5 nm. This ensures that, according to the criterion developed before, the (001) orientation should be only metastable. At a given temperature, the system is allowed to relax and after around 2×10^{-10} sec the system reaches equilibrium (the time step used is 1 fs). We illustrate this in Fig. 3 at $T = 300$ K for systems of initially $N_l = 20$, 16, and 12. The figure clearly shows the following: (i) (left panel) the absence of both surface or bulk reconstruction, with only a slight mismatch between the film and the annulus, (ii) surface reconstruction (middle panel) to an hexagonal arrangement, while the bulk of the film still retains its (001) orientation with some relaxation, and (iii) surface and bulk (filmwide) reconstruction appearing at the center of the sample film that relaxes to a (111) (layer by layer) orientation, as observed in experiments. A mismatch transition region is also seen, accommodating annular and bulk film lattice parameters. Surprisingly, for a similar diameter and $N_l = 8$ (~1.45 nm, the minimum critical thickness accomplished in experiments) a small thermal activation energy (~100 K) is required to achieve the transformation. Below such an energy barrier we observe the formation of large dislocations crossing the sample. We also evidenced that increasing the film diameter and preserving its thickness results in reduction of the required thermal activation energy for transformation. The existence of a finite energy barrier cannot be ruled out by the experiments, where local temperature was estimated

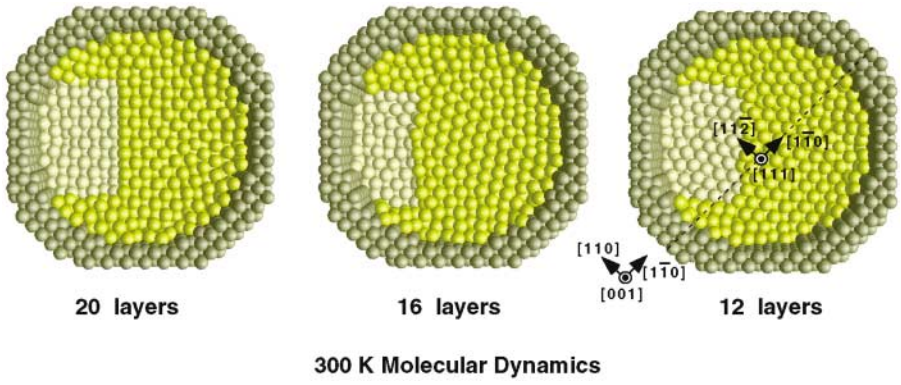

FIG. 3 (color). Top view of typical Au nanofilms configurations after equilibration at room temperature. Left, center, and right panels correspond to film of initially 20, 16, and 12 layers. Dark spheres at the borders correspond to frozen (001) atoms. The film atoms shown as gold and white correspond to the top and secondary layers, respectively. The (001) oriented border annulus and (111) oriented films are rotated relatively 35° around the $[\bar{1}10]$ axis bringing the [110] direction of the (001) film parallel to the $[11\bar{2}]$ direction of the (111) transformed film, as reported in experiments.

only as an upper bound (429 K), so thermal effects were excluded to within a few hundred degrees Kelvin.

A robust confirmation of the predictive nature of the simulation is the quantitative verification of the relative rotation between the fixed (001) boundary and the transformed (111) film. As reported in experiments, films (frozen and thinned) are rotated 35° around the $[\bar{1}10]$ with respect to one another. This brings the $[11\bar{2}]$ axis of the (111) parallel to the [110] direction. Such orientations are depicted in the right panel of Fig. 3 and are most likely related to a reduction of perimeter mismatch energy. The perimeter stresses, relaxed by a gradual interface between the transformed film and the fixed annulus, turn out only to decrease the energy barrier between the two crystalline configurations as compared to the situation with PBC conditions. This can be understood in terms of the nucleation of newly oriented material (see Fig. 3) at the center of the films to an extension such that it can meet the fixed boundary conditions [18].

Transformed film samples always contracted by approximately 5% with respect to their bulk counterparts. As in nanofilm experiments, we observe distributions of lattice spacings, but with a better defined average behavior. We recall that a contraction of 5% is consistent with a 5×20 surface reconstruction. This result supports the fact that the film transformation is initiated by the surface reconstructions; i.e., the resulting surface forces drive the change of the original structure inside the film.

We also implemented simulated thinning processes for other relevant metallic samples such as Al, Ag, Ni, and Pt. In all cases we were able to obtain the film transformation from (001) to (111). However, we evidenced that the required thermal activation energy strongly depends on the metal species. For samples of initial $N_l = 8$ and similar diameters as above, the transition occurs at approximately $T = 35 \pm 10$ K for Ag, 150 ± 25 K for Al, 600 ± 30 K for Ni, and 60 ± 20 K for Pt.

In summary, using the isobaric molecular dynamics simulations and the embedded atom method we are able to reproduce the structural transition from (001) to (111) in Au nanofilms observed in experiments at a critical film thickness. We show that this transition does not require high temperatures in agreement with experiments. Further results simulating Pt, Al, Ag, and Ni suggest that in suspended films the structural transition discussed is generic to other metal nanofilms. In contrast to surface reconstruction [12], the transformation can occur in $4d$ and $5d$ transition metals as well as in other metallic systems. We predict that the critical thickness for the transition should depend strongly on the surface area, a fact that could be checked experimentally. Obviously, it remains open to judge and validate our results from the point of view of electronic structures which can be achieved only by more fundamental *ab initio* methods [25]. These results may impact future developments in lithography techniques for nanodevice fabrication purposes.

Fruitful discussions with R. F. Angulo and P. A. Serena are acknowledged.

[1] E. Tossati and S. Prestipino, Science **289**, 561 (2000).
[2] W. A. de Heer, Rev. Mod. Phys. **65**, 611 (1993).
[3] R. N. Barnett and U. Landman, Nature (London) **387**, 788 (1997).
[4] M. Schmidt, R. Kusche, B. von Issendorff, and H. Haberland, Nature (London) **393**, 238 (1998).
[5] Y. Kondo and K. Takayanagi, Phys. Rev. Lett. **79**, 3455 (1997).
[6] D. Sánchez-Portal, E. Artacho, J. Junquera, P. Ordejón, A. García, and J. M. Soler, Phys. Rev. Lett. **83**, 3884 (1999).
[7] Y. Kondo and K. I. Takayanagi, Science **289**, 606 (2000).
[8] E. Tosatti, S. Prestipino, S. Kostlmeier, A. D. Corso, and F. D. Di Tolla, Science **291**, 288 (2001).
[9] A. I. Yanson, I. K. Yanson, and J. M. van Ruitenbeek, Nature (London) **400**, 144 (1999).
[10] A. Hasmy, E. Medina, and P. A. Serena, Phys. Rev. Lett. **86**, 5574 (2001).
[11] T. Wang, N. Moll, K. Cho, and J. D. Joannopoulos, Phys. Rev. B **63**, 035306 (2001).
[12] V. Fiorentini, M. Methfessel, and M. Scheffler, Phys. Rev. Lett. **71**, 1051 (1993).
[13] M. I. Haftel, Phys. Rev. B **48**, 2611 (1993).
[14] M. I. Haftel and M. Rosen, Phys. Rev. B **51**, 4426 (1995).
[15] V. A. Shchukin and D. Bimberg, Rev. Mod. Phys. **71**, 1125 (1999).
[16] M. Mitome, K. Takayanagi, and Y. Tanishiro, Phys. Rev. B **42**, 7238 (1990).
[17] J. A. Nieminen, Phys. Rev. Lett. **74**, 3856 (1995).
[18] Y. Kondo, Q. Ru, and K. Takayanagi, Phys. Rev. Lett. **82**, 751 (1999).
[19] Y. Mishin, D. Farkas, M. J. Mehl, and D. A. Papaconstantopoulos, Phys. Rev. B **59**, 3393 (1999).
[20] H. Mehl, O. Biham, I. Furman, and M. Karimi, Phys. Rev. B **60**, 2106 (1999).
[21] U. Landman, W. D. Luedtke, N. A. Burnham, and R. J. Colton, Science **248**, 454 (1990).
[22] M. Díaz, J. L. Costa-Krämer, P. A. Serena, E. Medina, and A. Hasmy, Nanotechnology **12**, 118 (2001).
[23] B. W. Dodson, Phys. Rev. Lett. **60**, 2288 (1988).
[24] T. A. Savas, M. Farhoud, H. I. Smith, M. Hwang, and C. A. Ross, J. Appl. Phys. **85**, 6160 (1999).
[25] A. Hasmy and E. Medina (to be published).